Journal of Catalysis **190,** 228–239 (2000)
doi:10.1006/jcat.1999.2747, available online at http://www.idealibrary.com on IDEAL®

Kinetics of the Selective Catalytic Reduction of NO over HZSM-5

Scott A. Stevenson,[1,2] James C. Vartuli, and Carlton F. Brooks[3]

Mobil Technology Company, Strategic Research Center, 600 Billingsport Road, Paulsboro, New Jersey 08066

Received April 26, 1999; revised October 29, 1999; accepted October 29, 1999

We have studied the kinetics of the selective catalytic reduction (SCR) of NO by NH_3 over HZSM-5. We find that between 350 and 450°C the reaction is first order in NO and oxygen concentration but is negative order in ammonia. The rate data can be modeled by assuming that ammonia inhibits the reaction by blocking sites necessary for NO oxidation, which appears to be the rate-determining step. Ammonia oxidation is measurable at all conditions studied and becomes increasingly important as temperature and oxygen concentration increase or as NO concentration decreases; the oxidation of ammonia is more likely to produce N_2 than NO. We have developed a kinetic model that accurately describes the rate of N_2 formation over a wide range of conditions. We suggest that the active site for NO oxidation may be highly acidic extra-framework aluminum rather than the framework Brønsted aluminum sites.

Key Words: **selective catalytic reduction (SCR); kinetics; HZSM-5.**

INTRODUCTION

The selective catalytic reduction (SCR) of nitric oxide by ammonia is the most widely used process for the reduction of NO emissions from combustion flue gas (e.g., 1). The generally accepted stoichiometry for this reaction involves the combination of equimolar amounts of NO and NH_3 in the presence of oxygen to produce nitrogen and water:

$$4NO + 4NH_3 + O_2 \rightarrow 4N_2 + 6H_2O.$$

Although a variety of materials show some catalytic activity for this reaction, catalysts based on mixtures of vanadia and titania are currently used in virtually all commercial SCR units. There has been significant interest, however, in developing zeolite-based catalysts. Zeolites offer a number of advantages over vanadia/titania catalysts: they are active over a wider temperature range, they are more resistant to thermal excursions, and the spent catalyst can present less of a disposal problem.

In spite of the interest in the reduction of NO by NH_3 over zeolite-based catalysts, there have been few studies of the kinetics or mechanism of the reaction over zeolites in the hydrogen form; the studies that have been published have focused on mordenite and ZSM-5 catalysts. Hirsch (2) examined the reduction of NO by NH_3 over H-mordenite at 400°C and found that the reaction was first order in inlet O_2 concentration. Increasing the NO_2/NO ratio in the feed increased NO_x conversion. When NO_2 was present in the feed, however, NH_3/NO_x ratios greater than 1 were required to achieve maximum NO_x conversion.

Andersson and co-workers (3–5) studied the SCR reaction over a series of catalysts prepared by the acid-leaching of H-mordenite. They observed that the rate decreased as the aluminum content decreased; the rates of NO oxidation to NO_2 and NO_2 reduction to NO were likewise found to correlate with aluminum content. The activation energy for NO reduction was determined to be approximately 14 kcal/mol for all samples. Because the amount of adsorbed NO^+ observed by FTIR correlated well with SCR activity, the authors suggested that it might be an important intermediate. Interestingly, they observed that as the NO_2/NO ratio was varied, the SCR rate went through a maximum when the concentrations of NO_2 and NO were roughly equal; it was suggested that both are required for the reaction. They proposed that the active site was a Lewis acid site formed from the dehydroxylation of a Brønsted acid site and that the rate-determining step was the oxidation of NO in the absence of NO_2 and the reduction of NO_2 to NO in the absence of NO. When both NO and NO_2 are present, it was suggested that they react to give NO^+ and NO_2^-.

Medros *et al.* (6) reported that the SCR reaction over H-mordenite is first order in NO. They observed an activation energy of 14 kcal/mol but drew no mechanistic conclusions.

Mastikhin and Filimonova (7) reported NMR observations of the reactions of NO, NH_3, and O_2 over HZSM-5, NaZSM-5, and silicalite at room temperature. Both the hydrogen and sodium forms of ZSM-5 were observed to be active; silicalite was inactive. They concluded that the key

---

[1] To whom correspondence should be addressed.

[2] Current address: SABIC Technology Center, 16200-A, Park Row, Houston, TX 77084. E-mail: scott.stevenson@sabicusa.com.

[3] Current address: Department of Chemical Engineering, Stanford University, Stanford, CA 94305-5025.

0021-9517/00 $35.00

step was the disproportionation of NO into NO_2 and N_2O, i.e.,

$$3NO \rightarrow NO_2 + N_2O,$$

and that the NO_2 species subsequently reacted with NO and adsorbed ammonia to give a surface species of the form $N_xO_y \cdot NH_3$, which then decomposed to give N_2.

Moon and co-workers (8) reported that the SCR reaction over HZSM-5 at 500°C was first order in NO concentration, −0.45 order in NH_3 concentration, and 0.77 order in O_2 concentration. Varying the temperature from 430 to 530°C increased the NO conversion rate only slightly, suggesting an apparent activation energy of less than 3 kcal/mol. They speculated that the rate-determining step in SCR over HZSM-5 is the reaction of NO with adsorbed oxygen to give adsorbed NO_2, which can then react with a surface ammonium ion to give an ammonium nitrite-like species.

Halasz *et al.* (9) studied the oxidation of NO to NO_2 over HZSM-5 and LiZSM-5 at temperatures ranging from 25 to 600°C. Because HZSM-5 was much more active than LiZSM-5 at 400°C, they concluded that the reaction took place on acid sites. They also observed that the reaction proceeded to equilibrium over HZSM-5 at 400°C and above; on this basis they concluded that NO oxidation could not be the rate-determining step in the SCR reaction.

Eng and Bartholomew (10, 11) studied the kinetics of NO reduction over several HZSM-5 and H-mordenite catalysts. They estimated the activation energy of N_2 formation to be 61 kJ/mol. They observed that the reaction was approximately first order in oxygen concentration, 0.73 order in NO concentration, and −0.61 order in ammonia concentration; the presence of up to 20% water in the feed was found to have little or no effect on the rate. They concluded that the observed inhibition of the SCR reaction by ammonia was caused by gaseous ammonia limiting the access of NO to adsorption sites within the zeolite and suggested that the rate-determining step was the oxidation of NO to NO_2 or NO^+. Because two samples with lower aluminum content showed little or no SCR activity, they proposed that the active site was a pair of neighboring Brønsted acid sites. Based on their kinetic data and the results of *in situ* FTIR studies, they postulated a reaction mechanism in which NO_2 reacts with two adsorbed ammonia molecules to give an adsorbed reaction intermediate that can further react with NO to give two molecules of N_2 or with NO_2 to give one molecule of N_2O and one of N_2.

A much larger literature exists describing the kinetics and mechanism of the SCR reaction over metal-exchanged zeolites (e.g., 12–24), due to the fact that the activity of these materials is generally much higher than that of the corresponding metal-free catalysts. A number of different mechanisms have been proposed for the various systems studied; it is interesting and often informative to consider these reports when studying results obtained over metal-free zeolites, although it is not always clear how or if the results are related.

As part of an effort to develop an effective zeolite-based catalyst for NO_x reduction we have studied the reaction of NO and NO_2 with NH_3 over a series of HZSM-5 catalysts. In this work we report our findings on the kinetics of NO reduction; in related publications we present data on the kinetics of NO_2 reduction (25) and the effect of sodium exchange and catalyst steaming on NO and NO_2 reduction activity (26).

METHODS

The catalyst used for this study was a sample of ZSM-5 with a nominal 27 : 1 silicon/aluminum ratio; elemental analysis suggested that the actual Si/Al ratio was approximately 22 : 1. The catalyst was prepared in the sodium form, exchanged with ammonium nitrate, and calcined to give the hydrogen form. Approximately 700 ppm sodium remained in the catalyst; this represents about 5% of the total aluminum content. The average crystal size, as measured by SEM, was estimated to be 0.50 μm. Before testing, the catalyst was dried *in situ* in flowing helium for 30 min at 100°C, at least 1 h at 150°C, and 2 h at 300°C; this pretreatment was found to be important in obtaining reproducible results.

Kinetic data were collected using a plug flow reactor operated in a downflow configuration; a bypass loop allowed the measurement of feed concentrations. A 0.46 g amount of ZSM-5, sized to 20/40 mesh, was loaded into a 3.49 mm inner diameter quartz tube reactor and held in place with quartz wool. The bed volume was approximately 0.81 cc. Oxygen, nitric oxide, and ammonia in balance helium, supplied from gas cylinders, were metered using mass flow controllers and mixed with helium at room temperature immediately before the reactor inlet to give the desired inlet concentrations. Trace amounts (2–15 ppm) of nitrogen were also present in the feed mixture and were properly accounted for in the mass balance. A total flow of 500 sccm was maintained, giving a space velocity of approximately 40,000 h^{-1}.

The catalyst was left on stream at each set of conditions for 3 h; a period of 60–90 min was generally sufficient for the catalyst to reach steady-state. The reactor effluent passed to the gas analyzers through a line heated to approximately 100°C; gas concentrations were recorded every 5 min. An MTI 200 gas chromatograph was used to determine O_2, N_2, and N_2O concentrations; calibrations were made using cylinders of known concentration supplied by Matheson. Two Siemens NDIR analyzers were used to measure NO and NH_3 levels; NO measurements made by this technique are more accurate than those made by chemiluminescence, which can be significantly affected by third-body quenching effects and interferences from other nitrogen-containing molecules, including ammonia (27, 28). Although the SCR reaction consumes equal amounts of NO and NH_3, under most conditions more NH_3 was converted than NO; we attribute this difference to ammonia oxidation, as discussed below. Material balances on atomic nitrogen were typically between 97% and 100%; the difference was attributed to NO_2 formation, which could not be detected with the analyzers available. In runs where oxidation of ammonia was negligible the amount of NO converted was slightly greater than the amount of NH_3 converted; this difference correlated well with the amount of NO_2 estimated from the mass balance.

Standard inlet conditions were 500 ppm NO, 500 ppm NH_3, and 1% O_2; variations to these concentrations were used to study the reaction kinetics. Temperatures were varied from 350 to 450°C. Blank tests showed no conversion of NO or NH_3 under these conditions. Within this temperature range, time on stream had no effect on catalyst activity or selectivity. Exposure to NO, NH_3, and O_2 at 500°C, however, caused irreversible changes in catalyst behavior.

The effect of deviations from differential conversions were accounted for according to the formula

$$r_{\text{true}} = r_{\text{meas}} \left(\frac{2r_{\text{inlet}}}{r_{\text{inlet}} + r_{\text{exit}}} \right), \qquad [1]$$

where r_{true} is the actual reaction rate at the inlet conditions, r_{meas} is the measured rate, r_{inlet} is the rate calculated from the kinetic expression using the inlet NO and NH_3 concentrations, and r_{exit} is the rate calculated from the kinetic expression using the NO and NH_3 concentrations measured at the reactor exit. This expression, while not exact, allows us to contend with the fact that the ammonia and NO concentrations do not decrease in a 1 : 1 stoichiometry and is a good approximation for conversions less than 50%, especially for net reaction orders of one or less. For the most part, NO conversions were less than 20% and NH_3 conversions were less than 30%. With the kinetic equation chosen to fit the data, as discussed below, the correction for nondifferential conversion did not exceed 8% for any single data point.

RESULTS

Apparent NO Order

Figure 1 shows the effect of changing inlet NO concentration on the measured nitrogen formation rate. (For this and all subsequent plots, the open points are the actual data and the solid lines are the kinetic fits to these data, according to the kinetic equation described below.) At all temperatures studied, the reaction rate varies linearly with NO concentration. This is in agreement with two previous studies of NO reduction on HZSM-5 and H-mordenite (6, 8); a third study (10) reported an NO reaction order of 0.73 when the inlet NO concentration was greater than the inlet NH_3 concentration but found the reaction to be zero-order in NO when inlet NO was less than inlet NH_3.

Although our data show that the rate of N_2 formation is linear in inlet NO concentration, the intercepts in Fig. 1 (i.e., the rates predicted in the absence of NO) are nonzero; both the slope and the intercept increase with increasing temperature. Even when no NO is fed, a significant amount of N_2 is formed. This suggests that some of the N_2 formation is due to the oxidation of ammonia.

Support for the hypothesis of ammonia oxidation and its contribution to the N_2 formation rate can be found by comparing the amount of NO and NH_3 converted at each set

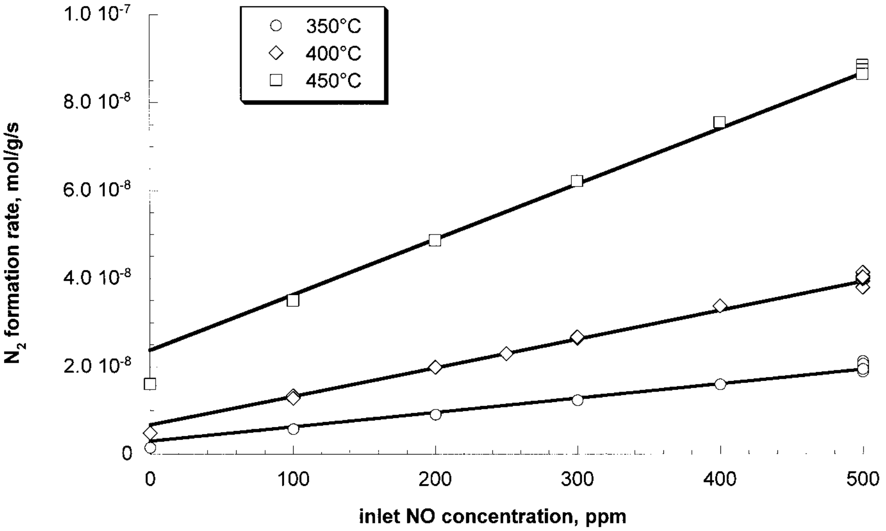

FIG. 1. Effect of inlet NO concentration on N_2 formation rate. Open points represent actual rate measurements; solid lines show results of kinetic fitting. Inlet conditions: $O_2 = 1\%$, $NH_3 = 500$ ppm. $T = 350$, 400, or 450°C as shown.

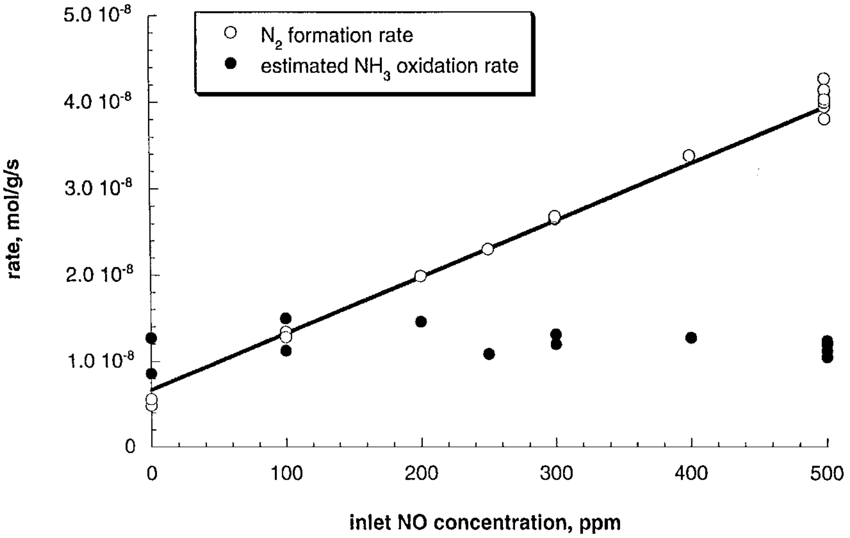

FIG. 2. Comparison of NH_3 oxidation by intercept and mass balance. See text for method of calculation of oxidation by mass balance. $T = 400°C$, inlet $NH_3 = 500$ ppm, inlet $O_2 = 1\%$.

of inlet conditions. For example, at 400°C with inlet concentrations of 500 ppm NH_3, 200 ppm NO, and 1% O_2, the measured exit NH_3 and NO_x concentrations are 449 and 189 ppm, respectively, indicating that the net ammonia conversion is 51 ppm vs a net NO conversion of only 11 ppm and suggesting that 20 ppm ammonia has been oxidized and subsequently converted to NO and N_2; this gives an ammonia oxidation rate of 1.5×10^{-8} mol/g/s. Likewise, when 500 ppm of NH_3, 1% O_2, and no NO were fed under these conditions, we observed 479 ppm NH_3, 7 ppm of N_2, and 7 ppm NO_x in the product stream; a simple mass balance indicates that 14 ppm of ammonia has been oxidized, a rate of 1.1×10^{-8} mol/g/s. Of this oxidized ammonia, 50% has been converted to N_2, a significantly higher fraction than the 5–10% of the inlet NO that is converted to N_2 under these conditions when NO is fed. Figure 2 shows that when this calculation is repeated for each data point collected at 400°C, 500 ppm NH_3, and 1% O_2, the estimated ammonia oxidation rate is independent of inlet NO concentration at approximately 1.2×10^{-8} mol/g/s. When compared with the total N_2 rate intercept of 0.7×10^{-8} mol/g/s, these data suggest that under these conditions approximately half of the ammonia oxidation leads to N_2 and half to NO. Similar calculations indicate that at 350°C with the same inlet conditions approximately half of the ammonia that is oxidized is converted directly to N_2, and that at 450°C this fraction exceeds 90%. Presumably an adsorbed, partially oxidized species is formed that can either desorb as NO_x or react with additional NH_3 to form N_2.

Figure 3 shows the effect of oxygen concentration on the relationship between SCR rate and inlet NO concentration. Again, we see that the N_2 formation rate varies linearly with inlet NO concentration but the rate in the absence of NO is non-zero. Additionally, we can see that increasing the inlet oxygen concentration increases the rate of N_2 formation. Interestingly, the rate of ammonia oxidation to N_2 appears to be relatively independent of oxygen concentration between 0.5 and 1.8% O_2.

Apparent Ammonia Order

The effect of variations in inlet ammonia concentration on the SCR rate is shown in Fig. 4. It is clear from the data that the reaction is inhibited by the presence of ammonia; even at low ammonia concentrations the observed SCR rate increases if less ammonia is fed. The degree of rate inhibition decreases as the temperature is increased, as would be expected if this inhibition were due to the competitive adsorption of ammonia. If the data are fit with a simple power law, the reaction order in ammonia decreases from approximately −0.55 at 350 and 400°C to −0.35 at 450°C; for comparison, Moon *et al.* (8) observed an ammonia order of −0.45 at 500°C, while Eng and Bartholomew (10) calculated an ammonia order of −0.61 for data collected between 340 and 425°C.

Apparent Oxygen Order

Figure 5 shows how changes in oxygen concentration affect the rate of N_2 formation. Between 0.5% and 2.0% oxygen, there is a linear relationship between oxygen concentration and the N_2 formation rate. Previous studies of SCR on H-form zeolites have reported oxygen orders of 0.77 to 1.06 (2, 8, 10). Linear fits to these data give non-zero y intercepts, a reasonable result if we remember that the rate of ammonia oxidation to N_2 was zero order in oxygen across this range (see Fig. 3.) Of course this does not imply that

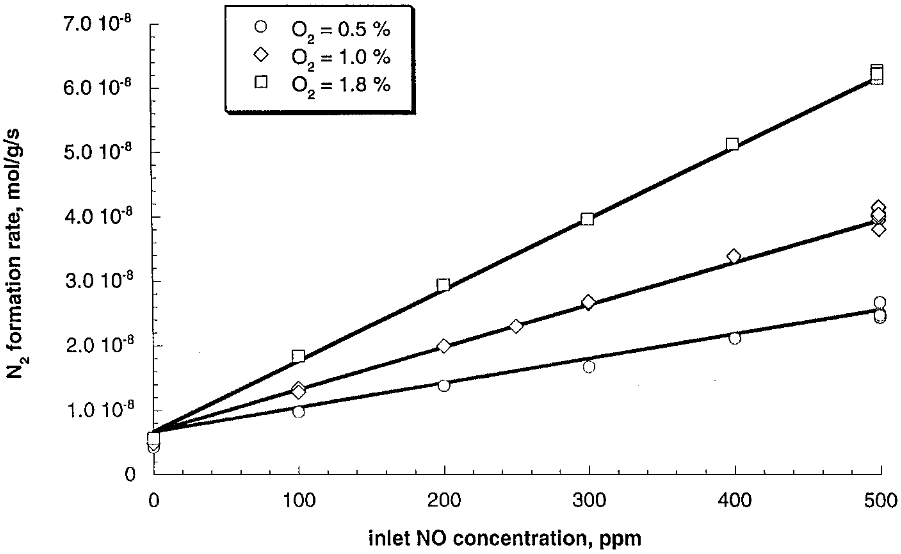

FIG. 3. Effect of inlet NO concentration on N_2 formation rate. $T = 400°C$. Inlet conditions: $NH_3 = 500$ ppm, $O_2 = 0.5$, 1.0, or 1.8% as shown.

the intercepts (shown by the dotted lines in Fig. 5) represent what the actual rate would be at zero inlet oxygen; it is likely that the rate in the absence of oxygen is zero or nearly so. What these intercepts represent is the contribution to the N_2 formation rate that is independent of oxygen concentration between 0.5% and 2.0% O_2, i.e., the "b" term in a linear fit, $y = mx + b$.

Figure 6 shows that the linear relationship between oxygen concentration and N_2 formation rate holds even at different inlet NO concentrations. Interestingly, the y intercepts of the linear fits to the data are dependent on the inlet NO concentration.

Modeling of Kinetic Data

In order to develop and refine our kinetic model, we employed an iterative approach: a kinetic form was assumed, the raw rate data were adjusted using these kinetic assumptions to account for deviations from nondifferential conversion, the corrected data were fit using an iterative least-squares approach to optimize the rate and adsorption constants, the assumptions were evaluated according to the quality of the fit, and the process was repeated until a satisfactory fit was found. Of course any kinetic model must agree with the observations presented above:

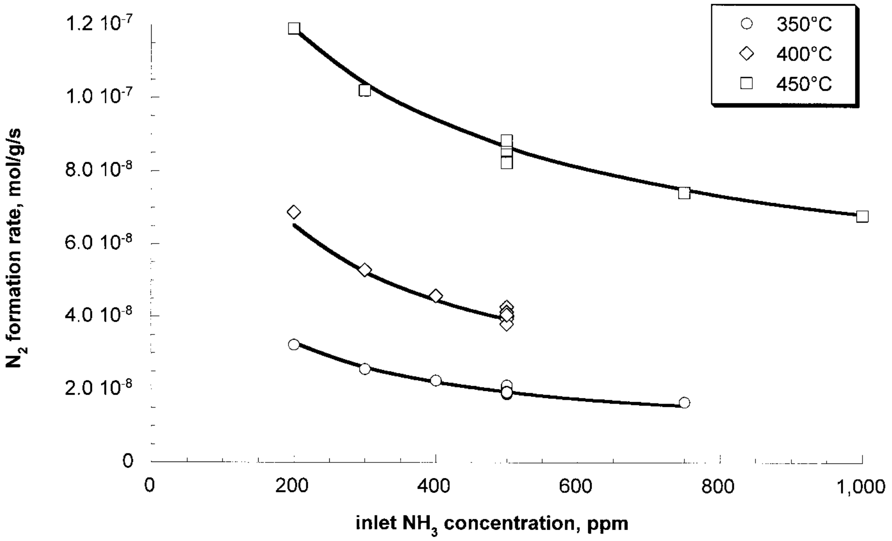

FIG. 4. Effect of inlet NH_3 concentration on N_2 formation rate. Inlet conditions: $O_2 = 1\%$, $NO = 500$ ppm. $T = 350$, 400, or 450°C as shown.

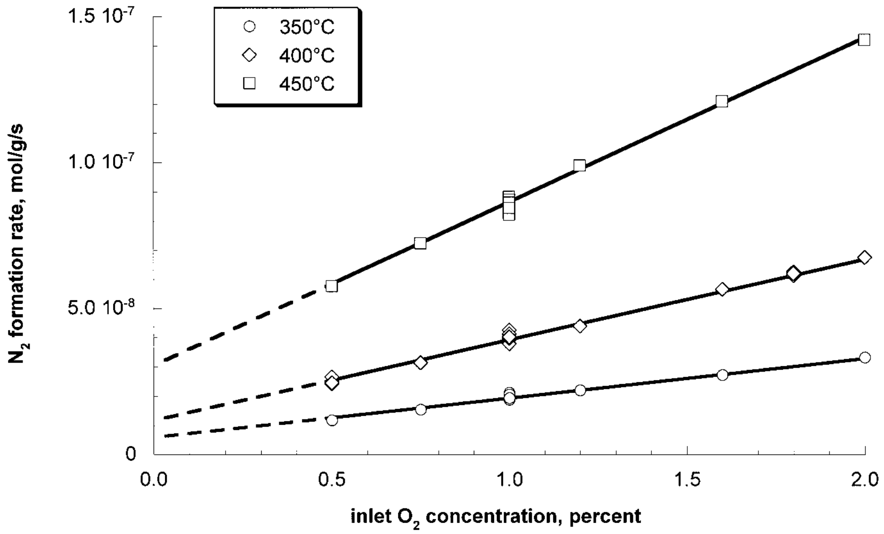

FIG. 5. Effect of inlet O_2 concentration on N_2 formation rate. Inlet conditions: NO, $NH_3 = 500$ ppm. $T = 350$, 400, or 450°C as shown. The *y* intercepts of dotted lines graphically show the magnitude of the oxygen-independent terms in the kinetic fits.

- The SCR reaction is first order in NO.
- The SCR reaction is inhibited by the presence of NH_3.
- The SCR reaction is first order in oxygen.
- The SCR reaction is partially masked by ammonia oxidation, which increases the rate of N_2 formation.
- The rate of ammonia oxidation is zero order in oxygen.

The most likely cause of rate inhibition by ammonia is competitive adsorption, i.e., ammonia is blocking sites needed for the reaction to take place. If ammonia adsorption and desorption are in equilibrium, the fraction of sites free of ammonia will be related to ammonia concentration by a Langmuir–Hinshelwood expression

$$\theta_* = \frac{1}{1 + K_a[NH_3]}, \qquad [2]$$

where θ_* is the fraction of sites available for reaction, $[NH_3]$ is the gas-phase ammonia concentration, and K_a is an adsorption constant. Since we observe the SCR rate to be first order in NO and O_2, the rate would then be given by

$$r_{SCR} = \frac{k_{SCR}[NO][O_2]}{1 + K_a[NH_3]}. \qquad [3]$$

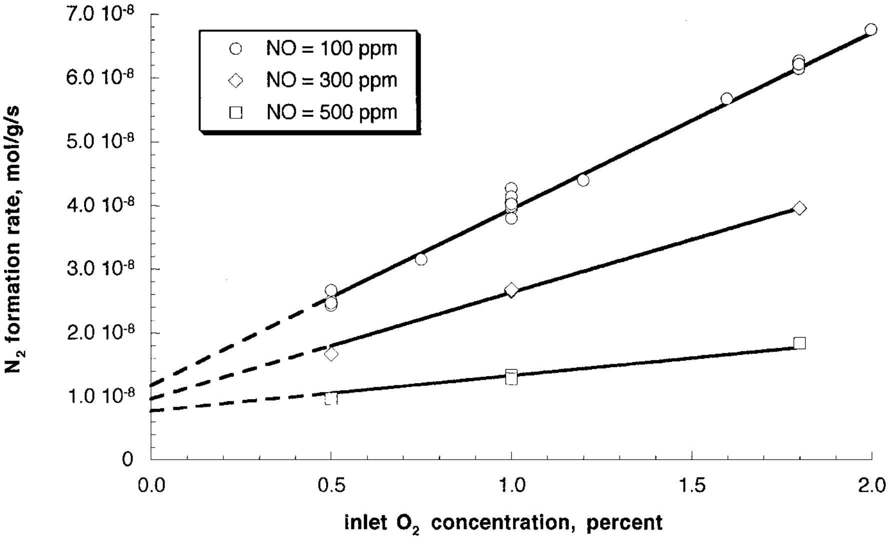

FIG. 6. Effect of inlet O_2 concentration on N_2 formation rate. $T = 400$°C. Inlet $NH_3 = 500$ ppm, inlet NO = 100, 300, or 500 ppm as shown. The *y* intercepts of dotted lines graphically show the magnitude of the oxygen-independent term in the kinetic fits.

If we assume that the rate of ammonia oxidation is a function of the ammonia coverage and is zero order in oxygen concentration, as observed, then the rate of nitrogen formation by ammonia oxidation, r_{ox}, is

$$r_{ox} = \frac{k_{ox} K_a [NH_3]}{1 + K_a [NH_3]}. \quad [4]$$

If ammonia oxidation and SCR took place on different sites, different adsorption constants would be used in Eqs. [3] and [4]; however, introducing this additional degree of freedom did not significantly improve the fits to our data.

Using Eqs. [3] and [4], a satisfactory fit to all the data can be obtained. However, fitting using these two terms alone gave a small, but consistent, offset from the data under certain conditions. This problem is most easily seen in the data presented in Fig. 6, where the y intercepts to the linear fits (represented by the dotted lines) are dependent on inlet NO concentration. By the logic of Eqs. [3] and [4], all of these y intercepts should be equal. (This extrapolation to zero inlet oxygen does not imply that the actual rate in the absence of oxygen is nonzero; it is only meant to graphically indicate the fraction of the rate that is independent of the oxygen concentration between 0.5 and 2.0% inlet oxygen, i.e., the "b" term in the linear fits, $y = mx + b$.) Similarly, if we compare the y intercepts in Figs. 1 and 5, which by the logic of Eqs. [3] and [4] should be equal, we find that they differ slightly: at 350°C, they are 0.23×10^{-8} and 0.57×10^{-8}, respectively; at 400°C, they are 0.62×10^{-8} and 1.14×10^{-8}; and at 450°C, they are 2.39×10^{-8} and 2.91×10^{-8} mol/g/s. In all cases, the intercept in Fig. 5 is greater than that in Fig. 1. A related difficulty becomes apparent if the slope of the data in Fig. 3 is plotted as a function of oxygen concentration; the relationship is linear but does not pass through the origin, as would be expected from Eqs. [3] and [4].

There are a number of possible explanations for these small discrepancies; the simplest and most successful in fitting the data is to assume that the SCR reaction occurs at a small but nonnegligible rate without the direct participation of oxygen. This rate is clearly first order in NO but is too small to accurately determine its dependence on ammonia concentration. Combining all three terms gives an overall rate expression of the form

$$r_{N_2} = \frac{k_{SCR}[NO][O_2]}{1 + K_a[NH_3]} + \frac{k_{ox} K_a [NH_3]}{1 + K_a [NH_3]} + k_o[NO]. \quad [5]$$

When 1% O_2 and equal amounts of NO and NH_3 are fed, approximately 65–70% of the total N_2 formation rate is due to the SCR reaction, 15–30% is due to oxidation of NH_3 to N_2, and 5–15% is due to the reaction of NO and NH_3 in the absence of O_2, depending on the temperature.

A number of variations on Eq. [5] were tried, especially with respect to the effects of oxygen and ammonia concentration, but none were found to give fits that were as good as this expression.

To further test our kinetic model, data were collected at a variety of different conditions. Figure 7 shows the effect of varying inlet NH_3 concentration at different oxygen concentrations; again we see that the N_2 formation rate is inhibited by ammonia. Figures 8 and 9 show the effect of varying the inlet NO and NH_3 concentrations together while maintaining a 1 : 1 molar ratio at different temperatures and inlet oxygen concentrations. Figure 10 shows that the rate varies linearly with inlet oxygen concentration even at lower inlet NO and NH_3 concentrations.

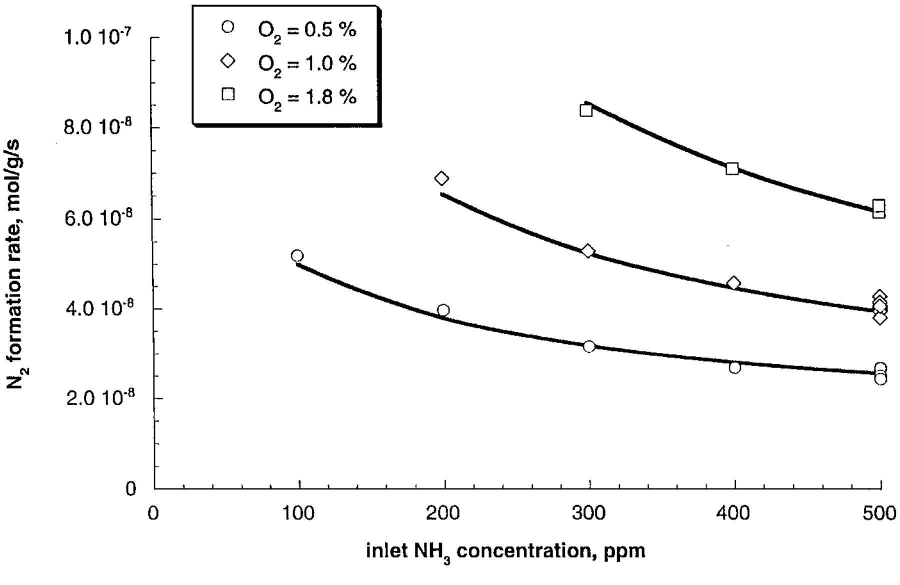

FIG. 7. Effect of inlet NH_3 concentration on N_2 formation rate. $T = 400$°C. Inlet conditions: NO = 500 ppm, O_2 = 0.5, 1.0, or 1.8% as shown.

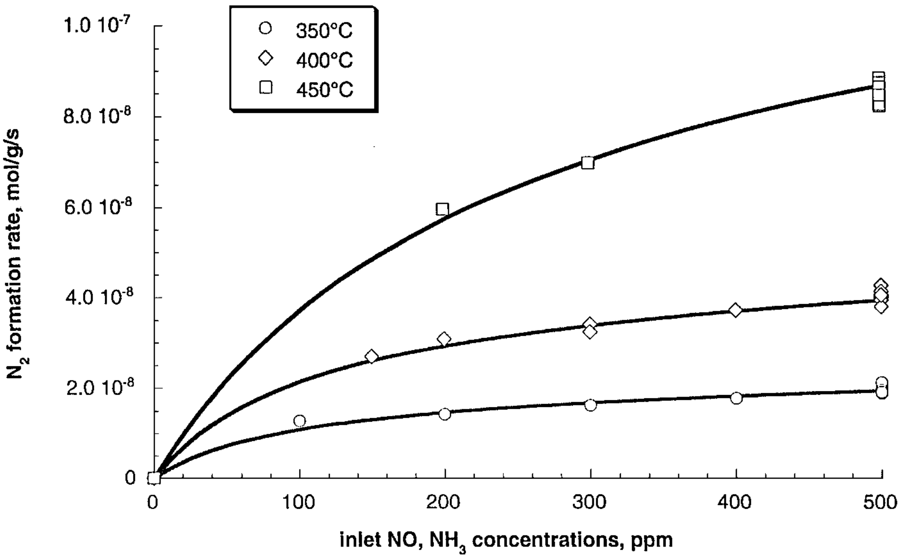

FIG. 8. Effect of varying inlet NO and NH_3 concentrations together in a 1:1 molar ratio. Inlet $O_2 = 1\%$, inlet $NO = NH_3$, $T = 350$, 400, or 450°C as shown.

The kinetic constants in Eq. [5] were optimized using a nonlinear quasi-Newton method to give the best fit to all of the data collected; the values giving the best fit are presented in Table 1. In total, 107 data points were fit; the average error was only 8.1×10^{-10} mol/g/s, or only 2.2% of the average rate. This error is equivalent to 1.1 ppm of N_2, which is within our experimental error. The quality of the fit is evident in Figs. 1 through 10, presented above; not only does the model accurately predict the rate at a wide variety of conditions but it also correctly describes the trends in the data as the inlet concentrations are varied. Confidence intervals (29) of 95% are also presented in Table 1. This error analysis supports the addition of the k_o[NO] term to the rate equation. The inclusion of this term is found to be significant at the 95% level at 400 and 450°C (i.e., $k_o = 0$ lies outside the confidence intervals); at 350°C, this term is found to be significant at the 90% level but not at the 95% level. It is also worth noting that the values of k_{scr} and K_a are highly correlated, since $K_a[NH_3]$ is much greater than unity.

Activation Energies

At our standard inlet conditions, we calculate an apparent activation energy for N_2 formation of 13 kcal/mol; this

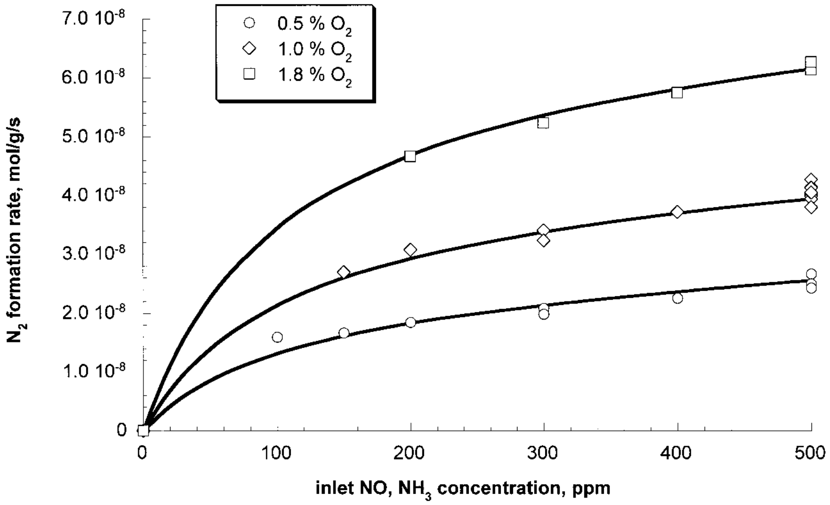

FIG. 9. Effect of varying inlet NO and NH_3 concentrations together in a 1:1 molar ratio. $T = 400$°C, inlet $NO = NH_3$, $O_2 = 0.5$, 1.0, or 1.8% as shown.

TABLE 1

Values of Kinetic Constants Used for Data Fitting*

T (°C)	k_{scr} (cm^6/mol/g/s × 10^{-7})	K_{a} (cm^3/mol × 10^{-8})	k_{ox} (mol/g/s × 10^9)	k_{o} (cm^3/g/s)
350	4.65 (3.7–7.3)	5.73 (3.6–11.0)	3.62 (1.6–5.9)	0.304 (–0.04–0.64)
400	9.85 (8.8–11.3)	5.36 (4.5–6.6)	8.11 (6.5–9.8)	0.558 (0.32–0.79)
450	12.7 (12.0–13.7)	2.64 (2.3–3.0)	34.4 (29–40)	0.807 (0.08–1.53)

* 95% Confidence intervals (29) are shown in parentheses.

is in excellent agreement with previous measurements of 14 kcal/mol over both H-mordenite (3,6) and HZSM-5 (10) but is significantly higher than the value of 3 kcal/mol reported by Moon *et al.* (8). However, the temperature dependence of the N_2 formation rate represents a combination of the temperature dependence of all three terms in Eq. [5]. The apparent activation energy of the SCR reaction is estimated to be 15 kcal/mol; of this, 9 kcal/mol is due to the SCR forward rate constant and the remainder is due to the decrease in the ammonia coverage as temperature increases.

Kinetics of N_2O Formation

Small amounts of nitrous oxide (up to 8.5 ppm, depending on the conditions) were detected whenever both NO and NH_3 were fed at 450°C or below. The amount of nitrous oxide produced rose as the temperature was increased from 350 to 400°C, but the amount observed at 450°C was less than at 350°C, and little or no nitrous oxide was detected at 500°C. The N_2O formation rate varied from approximately 22% of the N_2 formation rate at 350°C, to 13% at 400°C, and to only 4% at 450°C.

The most striking feature of the kinetics of nitrous oxide formation was that they were significantly different from the kinetics of N_2 formation. The N_2O formation rate was positive order in inlet ammonia concentration (see Fig. 11), rising from near zero order at 350°C to approximately 0.5 order at 450°C, and was less than first order in nitric oxide concentration, falling from 0.97 order at 350°C to 0.6 order at 400°C and to 0.5 order at 450°C. In contrast, the rate of N_2 formation varied linearly with NO inlet concentration and was negative order in NH_3 concentration. The rate of N_2O formation varied linearly with inlet oxygen concentration, as did the rate of N_2 formation.

DISCUSSION

Given the kinetic results described above, it is possible to draw some conclusions about the mechanism of the SCR reaction over HZSM-5. First, the inhibition of the rate by ammonia site-blocking suggests that ammonia does not participate in the rate-determining step under the conditions studied. This makes it unlikely that the combination of ammonia with NO is rate determining. In contrast, the rate is linearly dependent on NO concentration and strongly dependent on O_2 concentration. On the basis of these observations, we agree with previous suggestions (5, 8, 10) that the oxidation of NO to NO_2 or an adsorbed NO_2-like species

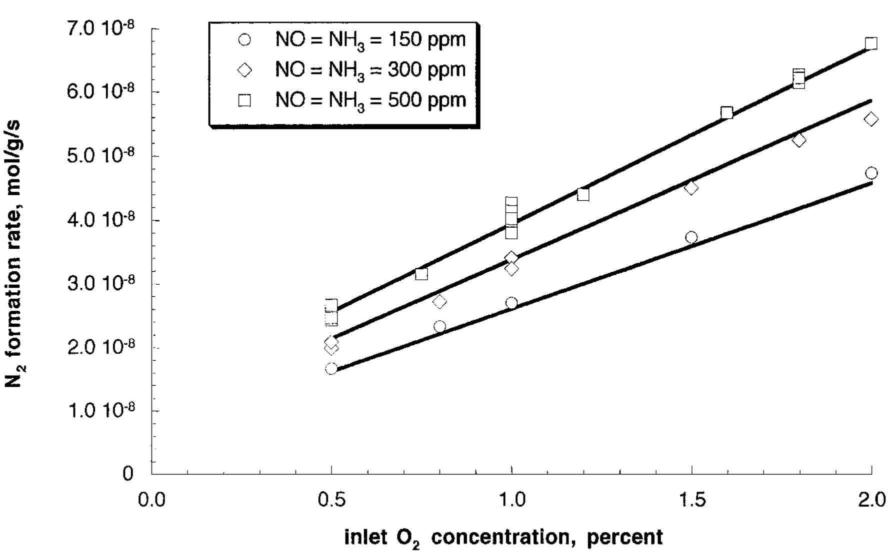

FIG. 10. Effect of inlet O_2 concentration on N_2 formation rate. $T = 400$°C. Inlet NO held in 1 : 1 molar ratio at 150, 300, and 500 ppm, as shown.

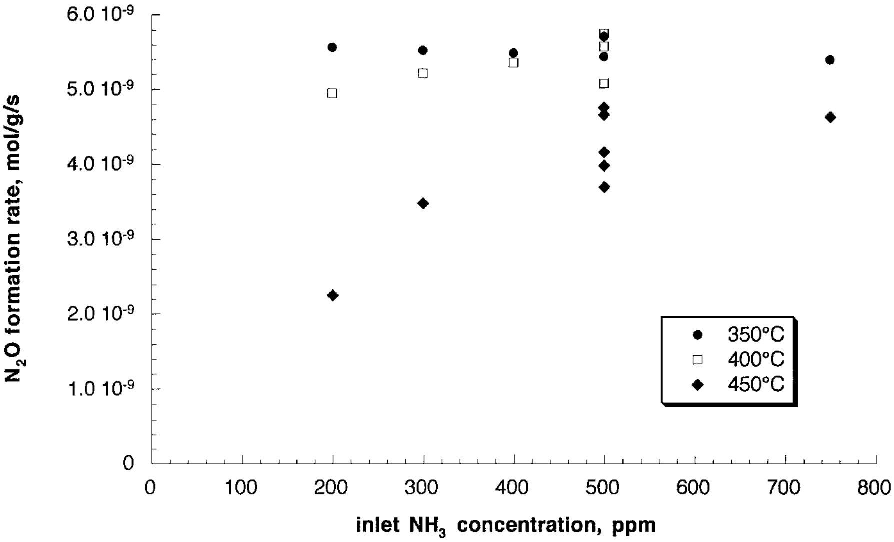

FIG. 11. Effect of inlet NH_3 concentration of N_2O formation rate. Inlet conditions: $O_2 = 1\%$, $NO = 500$ ppm. $T = 350$, 400, or 450°C as shown.

is the rate-determining step and that once adsorbed NO_2 is formed, it is rapidly converted to N_2 by reaction with NH_3.

$$NO + \tfrac{1}{2}O_2 \overset{\text{rds}}{\rightarrow} NO_2 \overset{\text{fast}}{\rightarrow} \text{products}. \quad [6]$$

Under reaction conditions, the sites needed for NO oxidation are in large part occupied by ammonia, which adsorbs much more strongly than NO or oxygen; this leads to the observed inverse relationship between inlet ammonia concentration and N_2 formation rate.

This conclusion is supported by two seemingly contradictory observations: in our SCR experiments, the gas exiting the reactor contains little NO_2, but we have found the same HZSM-5 catalyst to be active for the oxidation of NO to NO_2 in the absence of ammonia under the same conditions. Table 2 shows that 70–95 ppm NO_2 were formed when we fed 500 ppm NO and 1% O_2 over our catalyst at 300–400°C, but that less than 20 ppm exited the reactor when 500 ppm of ammonia was added to the inlet gas stream. If the NO oxidation data in Table 2 are used to calculate forward rate constants, correctly accounting for the effect of the reverse reaction on the conversion, the values estimated are 4.8×10^7 and 6.7×10^7 cm^6/mol/g/s at 350 and 400°C, respectively; these values compare well with the values of k_{scr} reported in Table 1. We also observed that the kinetics of the oxidation of NO to NO_2 in the absence of ammonia parallel the kinetics of the SCR reaction: NO oxidation is first order in NO and positive order in oxygen. These data are consistent with previous reports that HZSM-5 (9) and H-mordenite (5) catalysts converted NO and O_2 feeds to near-equilibrium mixtures at 400°C and above. Our observations are consistent with the hypothesis that ammonia slows the conversion of NO to NO_2 by blocking sites via adsorption and that most of the NO_2 that is formed is rapidly removed by reaction with NH_3 to give N_2.

It is interesting to speculate on what is the active site for NO oxidation. The obvious possibility is, of course, a zeolite Brønsted acid site. Halasz and Brenner (9) maintain that this is indeed the case, although their evidence is far from conclusive. However, the K_a values required to produce a good fit with the data correspond to relatively high ammonia coverages, ranging from approximately 35% at 450°C and 100 ppm ammonia to 85% at 350°C with 500 ppm ammonia. These coverages are significantly greater than those calculated from the calorimetric data of Sharma *et al.* (30) for HZSM-5 Brønsted acid sites (see Table 3 for comparison). Our observation of higher coverages suggests that acid sites stronger than the framework aluminum sites are necessary for this reaction to take place. From this, it is tempting to suggest that NO oxidation takes place primarily on the extra-framework aluminum cations, which are Lewis sites of higher acidity than the framework Brønsted sites (31). Sharma and co-workers estimated the heat of ammonia adsorption on these sites to be approximately 170 kJ/mol, which is larger than the 150 kJ/mol measured

TABLE 2

Conversion of NO to NO_2 over HZSM-5 in the Presence and Absence of NH_3[a]

T (°C)	NO_2 observed (ppm)		Equilibrium
	With NH_3	No NH_3	
300	0–3	74	336
350	0–6	93	220
400	15–20	86	124

[a] Inlet conditions: 1% O_2; 500 ppm NO; 500 or 0 ppm NH_3.

TABLE 3

Comparison of Estimated Ammonia Coverages for Active Site and Framework Aluminum Sites at 500 ppm Gas-Phase Ammonia

T (°C)	Active site fractional coverage	Framework sites fractional coverage[a]
350	0.85	0.69
400	0.83	0.20
450	0.69	0.04

[a] Data from Ref. (30).

on the Brønsted sites; sites of this increased strength would have high coverages similar to those predicted from the kinetic modeling. This suggestion that extra-framework aluminum is the active site for SCR on HZSM-5 is also supported by our data on the effects of sodium exchange and catalyst steaming on catalyst activity (26). However, this hypothesis is not consistent with the temperature dependence of the values of K_a presented in Table 1. Our estimate of the heat of adsorption obtained by plotting ln K_a vs $1/T$ is only 32 ± 13 kJ/mol; this value is much less than the heat of adsorption of ammonia on either the extra-framework or the framework aluminum sites. Because of this discrepancy, our suggestion that the extra-framework sites are the active sites for NO oxidation must remain tentative.

Eng and Bartholomew (10) have suggested that the active site for SCR over H-zeolites is a pair of neighboring Brønsted acid sites. However, this conclusion was based on their observation that an HZSM-5 sample with an Si/Al ratio of 35 showed no activity for SCR; they interpreted these results to suggest that below a certain aluminum content zeolites are not active for SCR. However, we have measured the SCR activity of a large number of HZSM-5 samples of varying aluminum content, with Si/Al ratios ranging from 12 to 350, and find that all have significant activity for this reaction; indeed, the rate does not correlate well with aluminum content. On the basis of these data, we do not believe that pair sites are necessary for this reaction.

It is clear from our data that although the SCR reaction is responsible for a majority of the N_2 formed over HZSM-5, the rate of ammonia oxidation is not insignificant. Although we are the first to quantitatively report the importance of ammonia oxidation, this reaction has been observed by others studying this reaction with H-zeolites. When feeding 700 ppm NH_3 and 2% O_2 over H-mordenite at temperatures from 310 to 425°C, Brandin and co-workers (4) reported ammonia conversions of up to 25%; N_2 was the only observed product. Moon and co-workers (8) observed that under normal SCR conditions, conversions of NO and NH_3 over HZSM-5 were unequal; they attributed this stoichiometry to the oxidation of ammonia to NO, N_2, or a combination of both. Eng and Bartholomew (10) state that ammonia oxidation appears to contribute slightly to the formation of N_2 and NO over their HZSM-5 sample, although it is difficult to quantitatively estimate the magnitude of this contribution since they do not measure ammonia conversion and have significant amounts of N_2 present in their feed gases. They observe that the N_2 formation rate is zero order in NO concentration when the inlet NO/NH_3 ratio is less than unity; this is most likely due to the large contribution of ammonia oxidation under these conditions. It seems likely that ammonia oxidation is important for most if not all H-zeolite catalysts. Presumably oxidation produces either NO_2 or another rapidly reduced species, since the majority of the ammonia oxidized appears to be converted directly to N_2 and not just to NO.

The presence of the third term in our rate equation (Eq. [5]) implies that the reduction of NO is possible without the direct participation of O_2. This should not be taken to imply that O_2 is not necessary for the reaction, only that in this pathway gas-phase oxygen does not participate in the rate-determining step or any step leading up to it. We believe it is possible that some NO may react directly with NH_3, or that some NO is being oxidized by oxygen atoms or hydroxyl groups associated with the zeolite framework. In any case, the contribution of this term to the overall N_2 formation rate is so small that no firm conclusions about the nature of this pathway can be drawn. It is worth noting that Eng and Bartholomew (10) also observe a small amount of conversion to N_2 in the absence of O_2.

One interesting implication of the strong rate inhibition by ammonia described above is that it suggests that a reactor with multiple ammonia injection points would result in much higher conversions than a process in which all of the ammonia was simply injected before the reactor entrance. Maintaining an average ammonia concentration of 100 ppm instead of 500 ppm would increase the rate of reaction by 50–100%, depending on the temperature.

SUMMARY

Our studies of the selective catalytic reduction of NO by NH_3 over an HZSM-5 catalyst show that this reaction is first order in nitric oxide and oxygen, but that the reaction is inhibited by the presence of ammonia. This inhibition can be most logically explained by the adsorption of ammonia on the active site. Although the temperature dependence of the estimated ammonia adsorption constant is much smaller than would be consistent with adsorption on an acid site, the degree of inhibition, especially at 400 and 450°C, suggests that ammonia is adsorbed more strongly than would be expected on the framework Brønsted acid sites. If this is the case, extra-framework aluminum is most likely the active site. The oxidation of NO to NO_2 proceeds rapidly in the absence of ammonia; similarities between the kinetics of NO oxidation and the SCR reaction suggest that NO oxidation is rate determining for SCR. Only a small amount of nitrous oxide is observed; the kinetics of N_2O

formation are quite different than the kinetics of N_2 formation, suggesting that this reaction occurs by a different pathway than SCR. Ammonia oxidation is slower than NO reduction but contributes measurably to the N_2 formation rate. We have collected data under a wide range of inlet NO, NH_3, and O_2 concentrations and at temperatures ranging from 350 to 450°C; we have developed a kinetic expression that accurately models these data, with an average error of only 2.2%.

ACKNOWLEDGMENTS

We acknowledge Sanjay Sharma, Dave Shihabi, Al Lang, and Phil Trotto for their helpful assistance and Mobil Technology Corporation for their support.

REFERENCES

1. Bosch, H., and Janssen, F., *Catal. Today* **2**, 1 (1987).
2. Hirsch, P. M., *Environ. Prog.* **1**, 24 (1982).
3. Andersson, L. A. H., Brandin, J. G. M., and Odenbrand, C. U. I., *Catal. Today* **4**, 173 (1989).
4. Brandin, J. G. M., Andersson, L. A. H., and Odenbrand, C. U. I., *Catal. Today* **4**, 187 (1989).
5. Odenbrand, C. U. I., Andersson, L. A. H., Brandin, J. G. M., and Järas, S., *Catal. Today* **4**, 155 (1989).
6. Medros, F. G., Eldridge, J. W., and Kittrell, J. R., *Ind. Eng. Chem. Res.* **28**, 1171 (1989).
7. Mastikhin, M. N., and Filimonova, S. V., *J. Chem. Soc., Faraday Trans.* **88**, 1473 (1992).
8. Moon, I. S., Namba, S., and Yashima, T., *Sekiyu Gakkaishi* **36**, 339 (1993).
9. Halasz, I., Brenner, A., and Ng, K. Y. S., *Catal. Lett.* **34**, 151 (1995).
10. Eng, J., and Bartholomew, C. H., *J. Catal.* **171**, 14 (1997).
11. Eng, J., and Bartholomew, C. H., *J. Catal.* **171**, 27 (1997).
12. Komatsu, T., Ogawa, T., and Yashima, T., *J. Phys. Chem.* **99**, 13053 (1995).
13. Komatsu, T., Nunokawa, M., Moon, I. S., Takahara, T., Namba, S., and Yashima, T., *J. Catal.* **148**, 427 (1994).
14. Nam, I.-S., Eldridge, J. W., and Kittrell, J. R., *in* "Catalysis (1987)" (J. W. Ward, Ed.), p. 589. Elsevier Science Publishers B. V., Amsterdam, 1988.
15. Ham, S.-W., Choi, H., Nam, I.-S., and Kim, Y. G., *Catal. Today* **11**, 611 (1992).
16. Ito, E., Hultermans, R. J., Lugt, P. M., Burgers, M. H. W., Rigutto, M. S., van Bekkum, H., and van den Bleek, C. M., *Appl. Catal. B* **4**, 95 (1994).
17. Kiovsky, J. R., Koradia, P. B., and Lim, C. T., *Ind. Eng. Res. Prod. Res. Dev.* **19**, 218 (1980).
18. Byrne, J. W., Chen, J. M., and Speronello, B. K., *Catal. Today* **13**, 33 (1992).
19. Chen, J. M., Speronello, B. P., Byrne, J. W., and Heck, R. M., "Kinetics of NO_x Reduction and Selective NH_3 Oxidation over a Honeycomb Catalyst," preprint 64 g, AIChE National Meeting, 1990, San Diego, CA.
20. Schmidt, R., Amiridis, M., Dumesic, J. A., Zelewski, L. M., and Millman, W. S., *J. Phys. Chem.* **96**, 8142 (1992).
21. Amiridis, M. D., Puglisi, F., Dumesic, J. A., Millman, W. S., and Topsøe, N. Y., *J. Catal.* **142**, 572 (1993).
22. Seiyama, T., Arakawa, T., Matsuda, T., Yamazoe, N., and Takita, Y., *Chem. Lett.* 781 (1975).
23. Mizumoto, M., Yamazoe, N., and Seiyama, T., *J. Catal.* **55**, 119 (1978).
24. Williamson, W. B., and Lunsford, J. H., *J. Phys. Chem.* **80**, 2664 (1976).
25. Stevenson, S. A., and Vartuli, J. C., in preparation.
26. Stevenson, S. A., and Vartuli, J. C., in preparation.
27. Winer, A. M., Peters, J. W., Smith, J. P., and Pitts, J. N., Jr., *Environ. Sci. Technol.* **8**, 1118 (1974).
28. Matthews, R. D., Sawyer, R. F., and Schefer, R. W., *Environ. Sci. Technol.* **11**, 1092 (1977).
29. Box, G. E. P., Hunter, W. G., and Hunter, J. S., "Statistics for Experimenters." John Wiley and Sons, New York, 1978.
30. Sharma, S. B., Meyers, B. L., Chen, D. T., Miller, J., and Dumesic, J. A., *Appl. Catal. A* **102**, 253 (1993).
31. Woolery, G. L., Kuehl, G. H., Timken, H. C., Chester, A. W., and Vartuli, J. C., *Zeolites* **19**(4), 288 (1997).